Biomass and Bioenergy 85 (2016) 207–214

Contents lists available at ScienceDirect

Biomass and Bioenergy

journal homepage: http://www.elsevier.com/locate/biombioe

Research paper

^{60}Co-γ radiation-induced changes in the physical and chemical properties of rapeseed straw

ChunYan Zhang [a, 1], XiaoJun Su [a, b, c, 1], XingYao Xiong [b, d], QiuLong Hu [b], Samuel Amartey [e], XingHe Tan [a, *], Wensheng Qin [f, **]

[a] College of Food Science and Technology, Hunan Agricultural University, Changsha 410128, China
[b] Hunan Provincial Key Laboratory of Crop Germplasm Innovation and Utilization, Hunan Agricultural University, Changsha 410128, China
[c] Hunan Collaborative Innovation for Utilization of Botanical Functional Ingredients, Hunan Agricultural University, Changsha 410128, China
[d] The Institute of Vegetables and Flowers, Chinese Academy of Agricultural Sciences, Beijing 100081, China
[e] Division of Biology, Imperial College of Science, Technology and Medicine, London E8 1PQ, UK
[f] Department of Biology, Lakehead University, Thunder Bay, Ontario P7B 5E1, Canada

ARTICLE INFO

Article history:
Received 22 June 2015
Received in revised form
23 November 2015
Accepted 25 November 2015
Available online 24 December 2015

Keywords:
Brassica napus L.
γ-ray irradiation
Microstructure
Reactivity

ABSTRACT

We investigated changes in the physical and chemical properties of rapeseed straw after treatment with different doses of ^{60}Co γ-irradiation (0 kGy-1200 kGy). Raman spectra, electron spin resonance (ESR), and nuclear magnetic resonance (NMR) analyses of the pretreated samples showed that the irradiation partially destroyed the intra- or intermolecular structure of rapeseed straw. Particle size distribution and specific surface area analyses suggested that irradiation decreased the particle size, narrowed the distribution range, and increased the specific surface area. Thermogravimetric analysis (TGA) and differential scanning calorimetry (DSC) curves showed that increasing the irradiated dose decreased the thermal stability of the treated rapeseed straw and increased the reactivity. Elemental analyses suggested that the oxygen content slightly increased, suggesting that oxygen in the air may be involved in the reaction. These results demonstrate that γ-irradiation can induce a series of changes in the physical and chemical properties of rapeseed straw.

1. Introduction

Lignocellulosic materials in straw, such as rapeseed straw, are insoluble. They have a compact structure and are made of high-molecular weight polymer compounds of high crystallinity, mainly, cellulose, hemicellulose, and lignin. The cellulose is wrapped in many layers of lignin and hemicellulose. The high crystallinity of cellulose fiber molecules prevents easy access by microorganisms and enzymes [1,2]. Under normal conditions, they are difficult to hydrolyze by chemical (acidic) or biological (enzymatic) catalysts. Effective pretreatments have to be used to disrupt the tight structure to make cellulose, lignin, and hemicellulose and to lose the structure of cellulose. Such pretreatments can increase the contact area of lignocellulose for subsequent effective hydrolysis by enzymes or chemicals.

Common pretreatment methods include mechanical milling [3], dilute acid/alkali treatment [4,5], steam explosion [6], ionic liquids [7], high-pressure liquid hot water [8], and high-energy ion irradiation [9]. These methods can effectively increase the accessible surface area of cellulose and thereby the sugar yield of enzymatic hydrolysis. The γ-rays from ^{60}Co can penetrate the fiber lattice to destroy the binding forces between carbohydrates and lignin in plant tissue. They can activate, as well as excite, molecules, eventually resulting in chain scission and depolymerization or chain cross-linking reactions [10]. Irradiation changes the physical, chemical, and biological characteristics of lignocellulose materials, making them easier to degrade further. The irradiation dose affects the degree of change of the structure of biomass [11]. Irradiated cotton cellulose has altered dynamical parameters due to intramolecular chain scission and depolymerization. When irradiated at a certain dose, the degree of polymerization (DP) in cotton cellulose drops, and the number of carbonyl increases [12,13]. After irradiation, the free radicals in the amorphous region quickly disappear, whereas those trapped in the crystalline and semi-crystalline

* Corresponding author.
** Corresponding author.
E-mail addresses: xinghetan@163.com (X. Tan), wqin@lakeheadu.ca (W. Qin).
[1] Authors contributed equally to this work.

http://dx.doi.org/10.1016/j.biombioe.2015.11.022
0961-9534/

regions remain longer and can cause further degradation of lignocellulose [14]. The degradation mechanism of rapeseed straw by radiation has not been reported. In this study, we investigated ^{60}Co-γ radiation-induced changes in the physical and chemical properties of rapeseed straw.

2. Materials and methods

2.1. Materials

Rapeseed straw (*Brassica napus L.*, variety Xiangyou 1358) was collected from experimental fields of the Institute of Oil Crops, Hunan Agricultural University, washed, dried at 60 °C for 5 days, and milled to pass through 40-mesh sieves.

2.2. Irradiation

Irradiation of the samples was conducted at the Nuclear Agricultural Sciences and Space Breeding Institute, Hunan Academy of Agricultural Sciences with a cobalt source of 9.99×10^{15} Bq. About 200 g of straw powder were placed in 1000 cm^3 jars and irradiated at 0 (CK), 400, 600, 800, 1000, and 1200 kGy at a dose rate of 2.0 $kGyh^{-1}$ at room temperature. The irradiated samples were stored at room temperature until further use.

2.3. Determination of particle size distribution and specific surface area

A laser particle size analyzer (Mastersizer 2000, Malvern, U.K.), using water as a dispersion medium and sodium hexametaphosphate as a dispersing agent, was used. An appropriate volume of water and sodium hexametaphosphate were added to the samples, mixed well by vortexing to ensure a uniform dispersion, and then loaded into the analyzer for simultaneous measurement of the particle size distribution and specific surface area.

2.4. Raman spectral analysis

Raman spectra were measured with a Nicolet Almega XR (Thermo Fisher, USA) with spectral resolution of 1 μm, an excitation power of 2 mW, and one time exposure of 10s. The samples were then dried and the dried samples were mounted on the stage for parallel scanning.

2.5. ESR scanning

The samples (20 mg each) were scanned with an ESR spectrometer (JES-FA200 cw-JEOL, Japan) in air at room temperature. An X-band was used at a frequency ranging from 8.8 to 9.6 GHz, with microwave power of 1 mW. The following were used: an initial field of 299 mT, a center field of 324 mT, a scan width of 50 mT, a modulation amplitude of 0.35 mT, a modulation frequency of 100 kHz, and a scanning time of 60s.

2.6. NMR

The samples (50 mg) were dissolved in 1 cm^3 D_2O (heavy water), and the NMR was measured directly using NMR spectroscopy AV400 (Bruker, Switzerland). The ^{13}carbon spectrum (^{13}C NMR) was detected with a tube diameter of 5 mm, rotation rate of 5 kHz, proton resonance frequency of 125.75 MHz, compensation time of 20 ms, contact time of 1 ms, and pulse delay time of 3 ms. Hydrogen spectroscopy (^{1}H NMR) NMR was detected with a proton resonance frequency of 600.1 MHz, π/2 pulse lengths of 2.57 μs, and a pulse delay time of 3 ms.

2.7. Elemental analysis

The composition of the straw was analyzed with a Vario EL III element analyzer (Elementar, Germany).

2.8. Thermogravimetric analysis (TGA)

The thermogravimetric properties of the straw powders before and after irradiation were assessed with a thermogravimetric analyzer TGA Q50 (Waters, USA), coupled with a DSC214 (Netzsch, Germany) analyzer. The carrier was high-purity N_2, with a flow rate of 50 cm^3min^{-1}. The heating rate was 30 °$Cmin^{-1}$ from room temperature to 1000 °C.

3. Results and discussion

3.1. Particle size distribution and specific surface area

The particle sizes, their distributions, and special surface areas are presented in Table 1 and Fig. 1. As shown, the Sautur mean diameter (D [3,2]), volume average particle diameter (D [4,3]), D (0.1), D (0.5), and D (0.9) decreased remarkably with increase of irradiation doses. For the nonirradiated sample, D [3,2] and D [4,3] were greater (127.092 and 1029.884 μm, respectively). The values obtained were 15.210 and 181.741 μm, respectively, after the samples were irradiated at 1200 kGy; D (0.1), D (0.5), and D (0.9) reduced from 90.578, 1182.345, and 1578.046 μm, respectively, before irradiation to 9.312, 52.981, and 594.083 μm, respectively, after irradiation at 1200 kGy. The reductions were dramatic, indicating that irradiation can reduce the particle size in a dose-dependent way. As the nonirradiated straw powders were screened through 40-mesh sieves, they had a uniform size distribution, with a clear and narrow main peak. However, the second peak was not obvious. The distributions of the samples subjected to low-dose radiation (400 and 600 kGy) were similar to those irradiated at CK. When irradiated at 800 kGy, the distribution had two peaks, suggesting that there were two dominant types of particles, each having a similar size. A further increase in the irradiation dose resulted in one strong peak, which increased with the dose, and a decreased second peak. The particle size distribution shifted toward smaller sized particles as the radiation dose increased. The higher the doses used, the greater the proportion of smaller particles. This indicates that the radiation strongly affected both the particle sizes and their distribution, possibly due to the destruction of the surface structure by chain scission and depolymerization during the irradiation, leading to increased brittleness and smaller sized particles. These results are consistent with those observed earlier [9].

The specific surface area is an important parameter of adsorbent, catalyst, and porous materials. Porous materials with high specific surface areas and activities often have strong high adsorption abilities. During the hydrolysis of cellulose, the enzymes must first be adsorbed onto the straw surface. Therefore, the specific surface area directly affects the outcome of enzymatic hydrolysis. Our results showed that in the nonirradiated sample, the specific surface area was 0.0472 m^2g^{-1}. With an increase in the irradiation dose, the specific surface area showed a clear upward trend and reached 0.394 m^2g^{-1} at the dosage of 1200 kGy. As the dose increased, the particle sizes decreased, and the specific surface area increased, inevitably increasing the accessibility of the enzymes during hydrolysis, thereby leading to more efficient hydrolysis. Beardmorel et al. [15] also found that the specific surface area of sulfite pulp was larger and that enzymatic hydrolysis was more efficient after irradiation.

Table 1
Particle size and specific surface area of rapeseed straw.

Irradiation doses (kGy)	Specific surface area (m^2g^{-1})	D[3,2]* (μm)	D[4,3]* (μm)	d(0.1)* (μm)	d(0.5)* (μm)	d(0.9)* (μm)
0	0.0472	127.092	1029.884	90.578	1182.345	1578.046
400	0.114	52.818	868.988	38.787	1086.828	1541.165
600	0.194	30.876	699.034	20.830	863.388	1484.602
800	0.319	18.800	371.846	12.154	81.695	1260.481
1000	0.387	15.513	251.576	9.500	53.276	982.774
1200	0.394	15.210	181.741	9.312	52.981	594.083

Note: D [3,2] is the Sautur mean diameter, D[4,3] is the volume mean particle diameter, d(0.5) is the median diameter, d(0.1) is the 10% diameter, and d(0.9) is the 90% diameter.

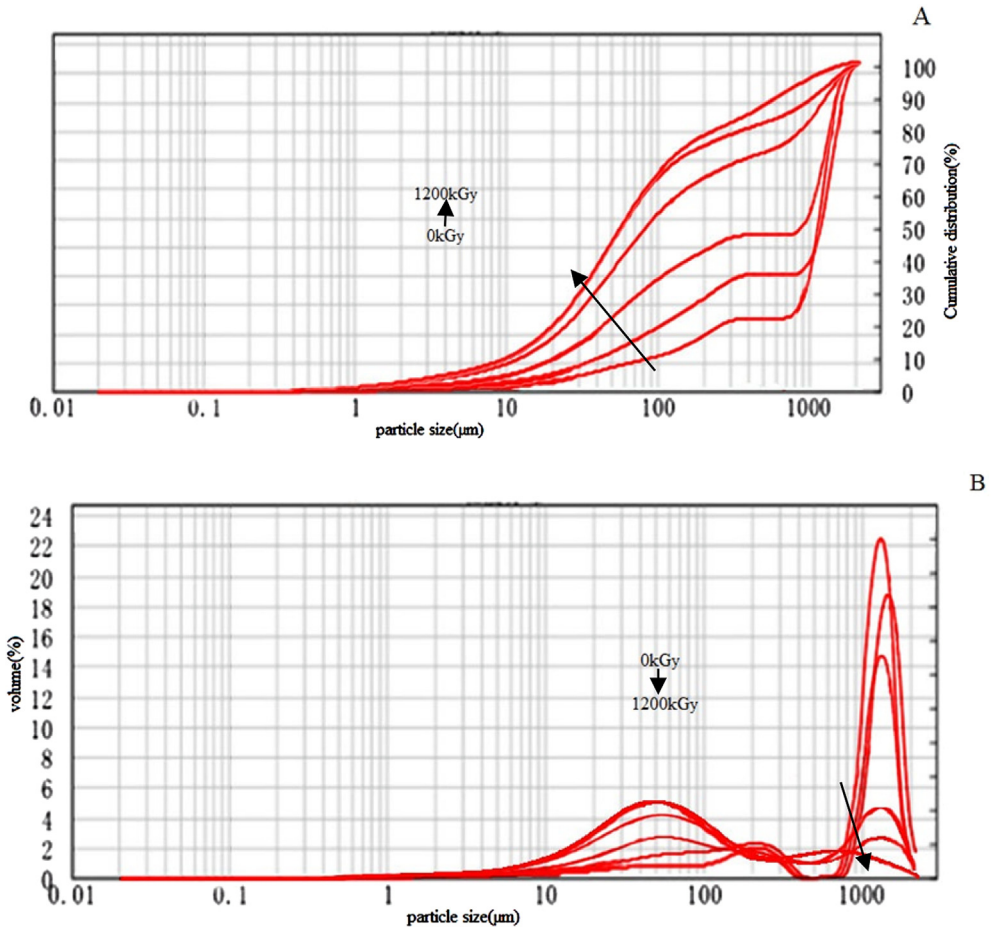

Fig. 1. The particle size distribution of rapeseed straw.

3.2. Raman spectra

The Raman spectra of the nonirradiated and irradiated straw samples are shown in Fig. 2, and their absorption bands are presented in Table 2. In the Raman spectra, there were three typical characteristic peaks for the cellulose fiber near 2901, 1094, and 376 cm^{-1}, representing the CH stretching vibration of CH and CH_2, asymmetric stretching vibration of glycosidic bond COC, and symmetric bending vibration of the pyranose ring CCC in cellulose. With an increase in the radiation dose, the intensity of the three peaks gradually decreased, suggesting that the radiation increased the damage to the straw fibers as the dose increased. Hemicellulose exists in amorphous form, but its chemical properties are similar to those of cellulose, and both have similar characteristic peaks. Therefore, the characteristic peak of hemicellulose may be masked by cellulose and difficult to identify. However, hemicellulose has a wider and weaker characteristic peak. In the straw samples, the two characteristic peaks of lignin were near 1649 and 1601 cm^{-1}. The 1649 cm^{-1} peak represents stretching vibration of C═C conjugated with the benzene ring in the coniferyl alcohol/sinapyl alcohol structure and C═O conjugated with the benzene ring in the coniferyl aldehyde/sinapyl aldehyde structure. The 1601 cm^{-1} peak represents symmetric stretching vibration of the benzene ring. The peak near 1649 cm^{-1} was not detected in all the non-irradiated samples, suggesting that the C═C and C═O bands were interrupted during irradiation. Meanwhile, the strength of the peak near 1601 cm^{-1} declined as the radiation dose increased, suggesting that the benzene ring was also damaged to some extent.

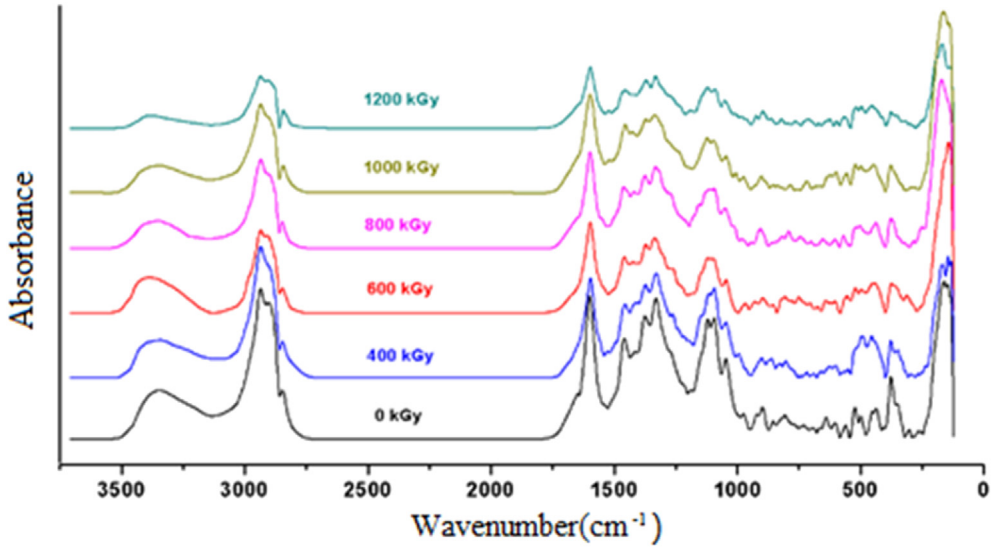

Fig. 2. The Raman spectra of rapeseed straw.

3.3. Free radicals

The concentrations of free radicals in the straw samples are shown in Fig. 3. As shown, there was a free radical signal in the non-irradiated samples, which might have resulted from the mechanical grinding and therefore it is called a mechanical free radical. The ESR spectra obtained from the irradiated straw were considerably different from the spectra obtained from the nonirradiated samples in terms of the curve shapes and width. The intensity of the spectra changed due to the superposition of the mechanical free radicals and free radicals induced by radiation. The peak height also increased with an increase in the dose applied. The free radicals mainly resulted from oxygen free radicals formed at C_1 or C_4 position of cellulose and lignin molecules after breakage of molecular bonds, followed by radicals generated in the polysaccharide components [16]. Therefore, the ESR spectra of rapeseed straw overlapped the ESR spectra of these radicals.

Table 2
Raman spectrum absorption band and assignment of rapeseed straw.

Wave number/ cm^{-1}	Characteristic peak
3348	OH stretching vibration
2800–3000	CH stretching vibration (including Chand CH_2 in methyl cellulose and lignin)
1649	Stretching vibration of C]O at the α position, conjugated with a benzene ring and Stretching vibration of C]C, conjugated with a benzene ring
1601	Symmetric stretching vibration of the benzene ring
1417	Deformation vibration of OCH_3 and shear vibration of CH_2
1200–1500	Bending vibration of HCC, HCO, HCH, and COH
1189	Rocking vibration of OCH_3
1119	Symmetric stretching vibration of the glycosidic bond COC
1094	Asymmetric stretching vibration of the glycosidic bond COC
1047	Stretching vibration of aromatic $-OCH_3$
950–1180	Stretching vibration of CC and CO (cellulose and hemicellulose)
899–1313	Stretching vibration of CH in αβ CH]CH
898	Plane symmetric stretching vibration of COC
609–727	Deformation vibration of benzene ring
603	Bending vibration of CCH
500–600	Bending vibration of the pyran ring COC
432–495	Skeleton bending vibration of the pyran ring COC
376	Symmetric bending vibration of pyran ring COC
<300	Bending vibration of the pyran ring COC and CO

During irradiation, polymer molecules in the straw samples are excited and ionized to produce chemical changes, resulting in breakage and decomposition of the polymer backbone and cross-linkage of polymers. As γ-rays have a strong penetrating ability, they can generate free radicals on the surface of and inside straw. In addition, due to the steric difficulties of large macromolecule free radicals generated during irradiation, the free radicals are unable to transfer within a long molecular chain or react with other molecules. Instead, the free radicals are stabilized by disproportionation or rearrangement reactions after chain scission [17]. As a result, the concentration and stability of free radicals generated by irradiation were higher than those in the nonirradiated samples.

3.4. NMR

NMR spectroscopy analysis is a very useful identification technique for analyzing the structure of the main chain and side chains in cellulose. Analysis of the ^{13}C NMR spectra can reveal directly the chemical environment of atom C [18]. To study the chemical structure characteristics of the straw, we analyzed its ^{13}C NMR and ^{1}H NMR spectra (Figs. 4 and 5). C spectra is in Fig. 4, In the C spectra, C_6 at the main hydroxyl groups was assigned to the peak with a

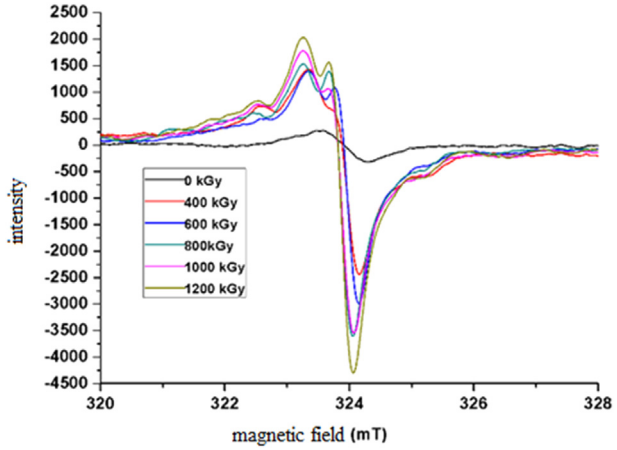

Fig. 3. The ESR spectra of rapeseed straw.

chemical shift of 64.9 ppm; C_2, C_3, and C_5, which were not connected to glycosidic bonds, were assigned to the peak with a chemical shift of 88.8 ppm; C_1 was assigned to the peaks with a chemical shift of 105.1 ppm.

The signal peak at 172.4 ppm was assigned to the carbonyl in hemicellulose acetyl. The signals of the peaks with chemical shifts of 74.8 and 64.9 ppm were relatively clear, each corresponding to C_3 and C_5 in 1, 4-β-D xylose, suggesting that the straw fiber has a higher xylose content.

The signal of the aromatic region in lignin generally appears between 104 and 168 ppm, and the signal in this region is helpful to determine the structural characteristics of the benzene ring in the large lignin molecule. In the signal regions of aromatic residues, the chemical peak shifts of the G structure unit were 112.2 ppm (C_2 structure), 114.9 ppm (C_5 structure), 118.5 ppm (C_6 structure), 134.3 ppm (C_1 connected by an ether bond), 145.4 ppm (C_4 connected by a non-ether bond), 147.4 ppm (C_3 connected by an ether bond), and 150.2 ppm (C_3 connected by an ether bond). The shifts in the S structure unit were 105.1 ppm (C_2/C_6 structure), 133.0 ppm (C_1 connected by a non-ether bond), 134.3 ppm (C_1 connected by a non-ether bond), 138.4 ppm (C_4 connected by an ether bond), 152.9 ppm (C_3/C_5 structure connected by an ether bond), 56.2 ppm (guaiacyl syringyl or $-OCH_2$), 72.3 ppm (C_α structure connected by a β-O-4 connection unit), 62.8 ppm (C_γ(β1,β5,β-O-4′),C_α/C_β structure), 129.9 ppm (C_1 structure in β_5), and 146.5 ppm. (C_3/C_5 in a non-ether bond connected to β-O-4′). The presence of these structures indicates that rapeseed straw lignin has a typical structure of dicotyledonous plants and that it contains mainly G-S-type lignin, with guaiacyl-syringyl residues. The C at the α, β, and γ positions of propyl in the main structural units (guaiacyl and syringyl) formed C—C and C—O structures with C of the benzene ring via different chemical bonds, such as β1, β5, and β-O-4′.

In addition, 114.9 ppm (C_3/C_5 in *p*-coumaric acid ester), 125.8 and 125.1 ppm (C_1 in *p*-coumaric acid ester), 129.9 ppm (C_2/C_6 in *p*-coumaric acid ester), 144.3 ppm (C_α and C_β *p*-coumaric acid ester), 159.0 ppm (C_4 in *p*-coumaric acid ester), and 168.4 ppm (C_γ in *p*-coumaric acid ester) were all derived from *p*-coumaric acid esters. These signals were very strong, suggesting that the rapeseed straw contains a higher content of coumaric acid ester. However, the latter was not detected by the GC—MS analysis, suggesting that irradiation did not disrupt the ester bonds between the *p*-coumaric acid and lignin. The concentration of C_6 and C_γ in the ester bond-connected ferulic acid was 122.0 ppm and 168.4 ppm, respectively. These findings indicate that lignin in rapeseed straw is linked to *p*-coumaric acid via an ester bond and to ferulic acid via an ether bond.

After irradiation, the signal of carbon atom corresponding to the glucosyl unit in cellulose was significantly decreased, an indication of dramatic cellulose degradation, whereas there was very little change in the peak corresponding to lignin. This finding suggests that lignin is not sensitive to irradiation. It is reasonably explained that the basic structure unit of lignin is phenyl propane, and its main chain is not easily be damaged in the radiation condition, whereas the β-1,4-glucosidic bond of the basic structure unit in cellulose is more easily damaged by radiation. But for hemicellulose, due to the overlap of peaks with that of cellulose, it is difficult to give a meaningful interpretation.

The ^{1}H NMR spectra of the rapeseed straw are shown in Fig. 5. The chemical shifts of 4.2 and 5.4 ppm were proton signal peaks of hemicellulose. The proton signal peak for the sugar ring was at 4.2 ppm, which was dramatically reduced with an increased radiation dose. The chemical shifts of anomers in hemicellulose were between 4.3 and 5.6 ppm. The anomer hydrogen can be divided into two sub-regions to distinguish the type of glycosidic bond connections. The proton region of the anomer at 5.4 ppm was an α-anomer. The major glycosidic bonds connecting the surface hemicellulose glycosidic bonds were α-glycosidic bonds. The peak intensity at 4.41 ppm decreased remarkably with an increased radiation dose, whereas the intensity at 1.48 ppm increased with an increasing irradiation dose until 1200 kGy and then decreased. All the peaks were shifted to the right at this dose. This may be due to an increase in the hydrogen proton in the low dose range

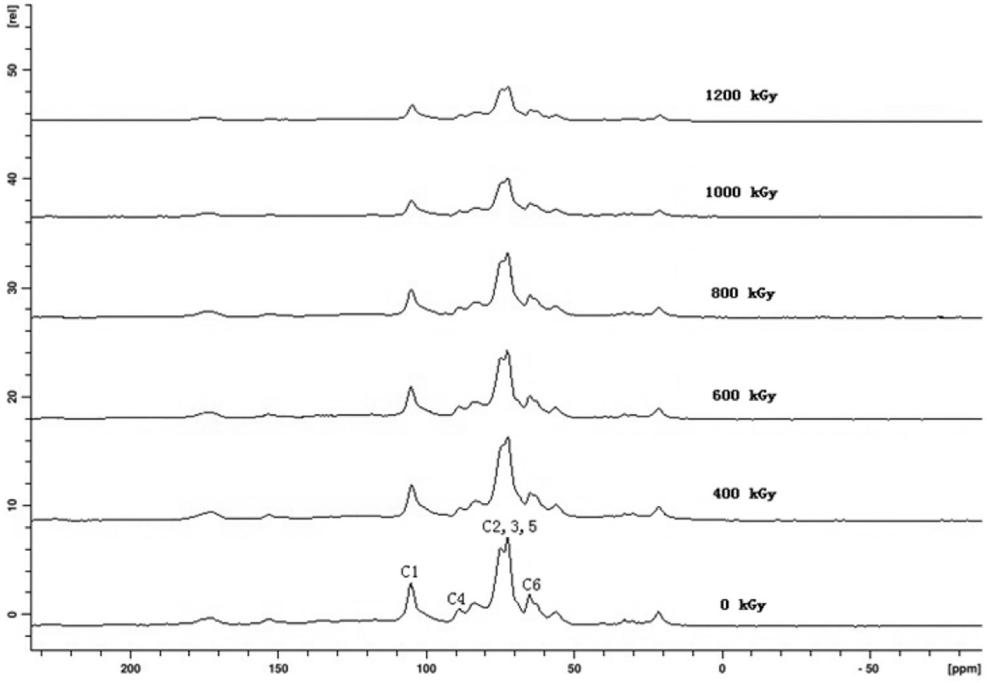

Fig. 4. The ^{13}C NMR spectra of rapeseed straw.

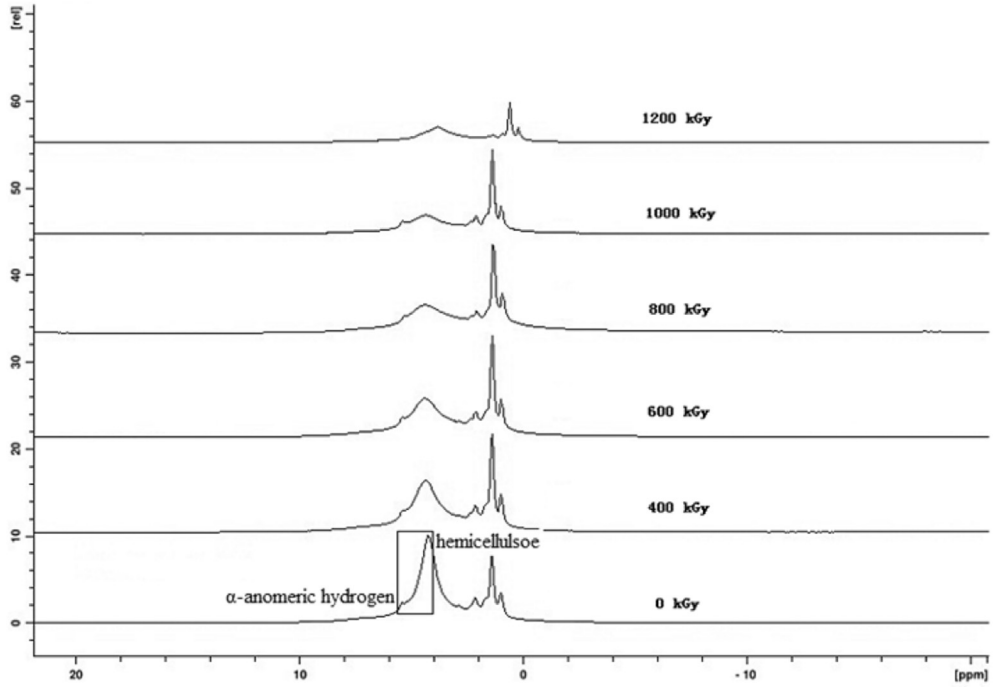

Fig. 5. The ^{1}H NMR spectra of rapeseed straw.

(1000 kGy), when the irradiation dose increased to 1200 kGy, the hydrogen proton took part in oxidation reaction, this was pointed to a substantial decrease of it, so its peak intensity decreased and shifted to the right.

3.5. Elemental analysis

The results of the elemental analysis of the rapeseed straw samples before and after irradiation are presented in Table 3. It is clear that the straw consisted of three major elements: C, H, and O. No visible changes in C, H, N, and S were observed before or after irradiation, although the content of O increased slightly when the irradiation dose was increased from 45.39% (nonirradiated) to 47.44% (irradiated) at 1200 kGy. This could be due to oxidation reactions between air oxygen and some substances in the straw during irradiation.

3.6. Thermogravimetric analysis

The TG, differential thermal gravity (DTG), and DSC curves of the straw powder before and after irradiation are shown in Fig. 6. As can be seen from the TG curves in Fig. 6A, the trend of change in the three curves is similar. Pyrolysis of rapeseed straw involves several stages. In the first stage, water is evaporated from the straw, and there is a slight (less than 10%) weight loss; in the second stage, polymers, mainly hemicellulose, are degraded. In this stage, the sample is depolymerized, and "vitrification" occurs [19]; in the third stage, cellulose and lignin are degraded. In this stage, pyrolysis takes place. The decomposition of the sample during this stage results in the generation of condensable, volatile large and small molecules, leading to heavy weight loss. In the fourth stage, when the temperature exceeds 400 °C, lignin degradation continues, and the residues are slowly decomposed to form charcoal and ash. Among the three major components of lignocellulosic materials, hemicellulose has the worst thermal stability. Therefore, thermal decomposition begins with the decomposition of hemicellulose (at about 200 °C). At 400 °C, the weight loss is about 70%. In the later stage, lignin is degraded continuously until 800 °C, leaving about 20–30% of residue.

As can be seen from the DTG curves in Fig. 6B, the nonirradiated rapeseed straw started to decompose at 20 °C. As the radiation dose was increased, the temperature at which weight loss began decreased gradually from 170 °C at 400 kGy to 140 °C at 1200 kGy, indicating that irradiation reduced the thermal stability of the straw. With an increase in the radiation dose, the reaction reached the maximum rates at temperatures of 320.8 °C, 263.5 °C, 258.4 °C, 253 °C, 251.7 °C, and 248.7 °C, respectively. Thereafter, the temperature at which the maximum reaction rate reached was declined. This implies that the reactivity of the rapeseed straw increased after irradiation. This was probably due to irradiation-induced damage of the straw structure and increased production of free radicals.

From the DSC curves in Fig. 6C, it is clear that pyrolysis is an endothermic to exothermic transformation process. At the beginning of the process, heat is absorbed. The samples are then quickly pyrolyzed to release a lot of the heat. In the present study, the heat absorbed and released from the nonirradiated samples was significantly higher than that of the irradiated samples. This might be due to irradiation-induced destruction of the straw structure and irradiation-induced breakage of some chemical bonds,

Table 3
Elemental analysis of rapeseed straw.

Irradiation doses (kGy)	C	H	N	S	O
0	40.97%	5.60%	1.09%	0.80%	45.39%
400	41.05%	5.65%	1.11%	0.77%	45.98%
600	41.00%	5.45%	1.11%	0.72%	46.17%
800	41.13%	5.68%	1.12%	0.72%	46.52%
1000	41.07%	5.46%	1.10%	0.71%	46.96%
1200	40.98%	5.47%	1.13%	0.72%	47.44%

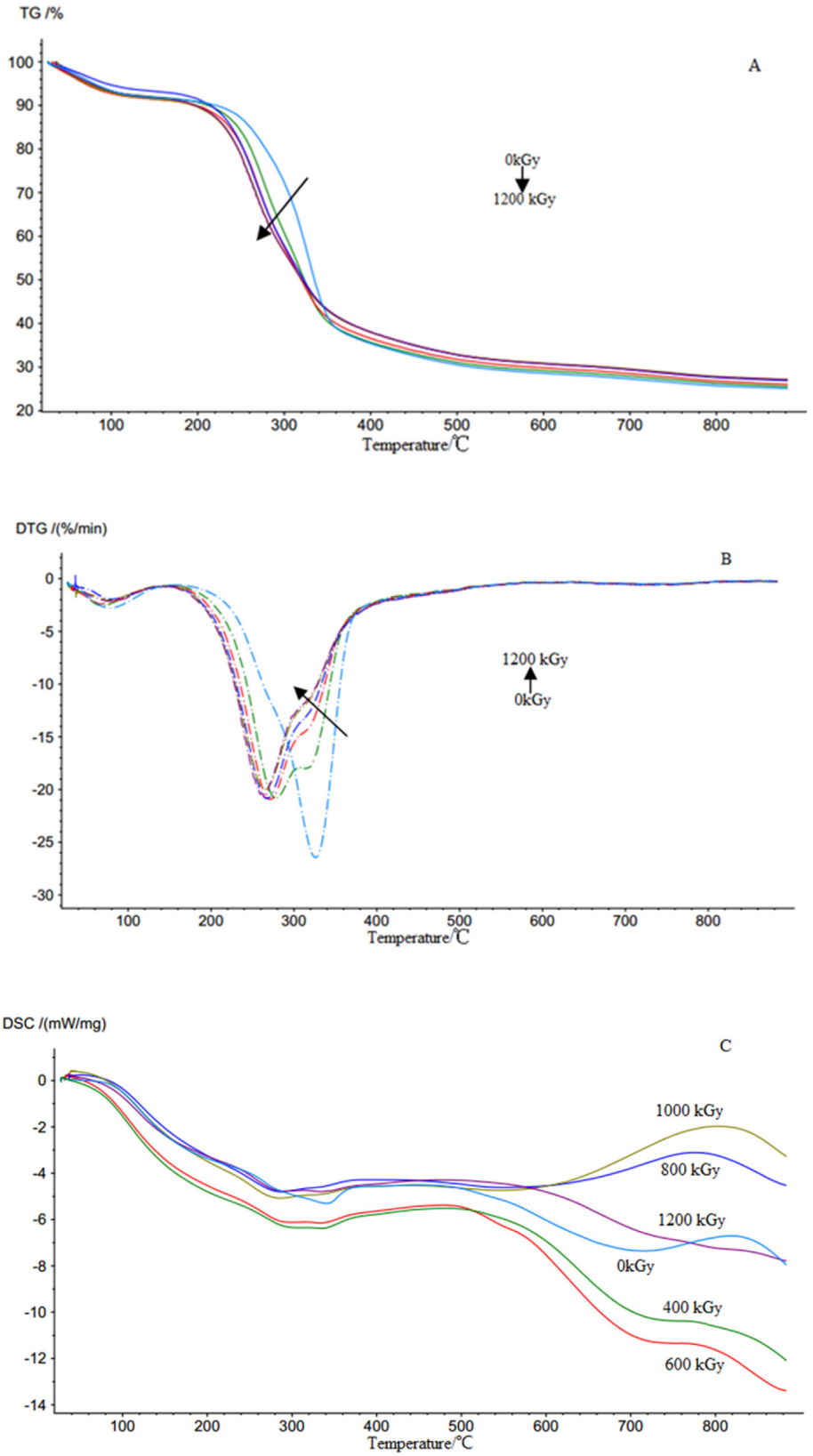

Fig. 6. Effects of irradiation doses on the thermogravimetry of rapeseed straw.

reducing the endothermic and exothermic ability of irradiated samples.

4. Conclusion

Chain scission and depolymerization during irradiation damaged the surface structure of rapeseed straw, resulting in smaller-sized particle and an increased specific surface area. As a result, some intra- and intermolecular bonds of the lignocellulose were broken, leading to decreased thermal stability, increased reactivity, and increased amounts of free radicals. The O content of the irradiated straw was slightly increased due to a reaction with air oxygen. To sum up, irradiation results in a series of changes in the morphology and molecular structure of lignocellulosic materials.

Acknowledgments

This study was supported by the National “863” Program of High Technology Research and Development of China (2012AA101804) and the Science and Technology Project of Hunan Province, China (2015NK3009).

References

[1] M.J. Taherzadeh, K. Karimi, Pretreatment of lignocellulosic wastes to improve ethanol and biogas production: a review, Int. J. Mol. Sci. 9 (9) (2008) 1621–1651.
[2] F.A. Khan, Radiation-induced Graft Copolymerisation and Characterisation of Jute Fibre, Cranfield University, U.K., 1999. Ph.D. Thesis.
[3] J.P.H. Van Wyk, A.M. Mogale, T.A. Seseng, Bioconversion of wastepaper to sugars by cellulase from Aspergillus niger, Trichoderma viride and Penicillium funiculosum, J Solid Waste Technol. Manag. 27 (2001) 82–86.
[4] Y. Sun, J.J. Cheng, Dilute acid pretreatment of rye straw and bermudagrass for ethanol production, Bioresour. Technol. 96 (14) (2005) 1599–1660.
[5] X. Zhao, L. Zhang, D. Liu, Comparative study on chemical pretreatment methods for improving enzymatic digestibility of crofton weed stem, Bioresour. Technol. 99 (9) (2008) 3729–3736.
[6] E. Ruiz, C. Cara, P. Manzanares, Evaluation of steam explosion pretreatment for enzymatic hydrolysis of sunflower stalks, Enzyme Microb. Technol. 42 (2) (2008) 160–166.
[7] D.B. Fu, G. Mazza, Aqueous ionic liquid pretreatment of straw, Bioresour. Technol. 102 (13) (2011) 7008–7011.
[8] D. Nabarlatz, A. Ebringerova, D. Montane, Autohydrolysis of agriculture by-product for the production of xylo-oligaccharides, Carbohydr. Polym. 69 (1) (2007) 20–22.
[9] G.S. Yang, Y.P. Zhang, M.Y. Wei, H.L. Shao, X.C. Hu, Influence of γ-ray radiation on the structure and properties of paper grade bamboo pulp, Carbohydr. Polym. 81 (2010) 114–119.
[10] E. Eakacs, L. Wojnarovits, J. Borsa, C.S. Foldvary, P. Hargittai, O. Zold, Effect of γ-irradiation on cotton-cellulose, Radiat. Phys. Chem. 55 (1999) 663–666.
[11] C.P. Yang, Z.Q. Shen, Y. Guoceb, J.L. Wang, Effect and aftereffect of γ radiation pretreatment on enzymatic hydrolysis of wheat straw, Bioresour. Technol. 99 (2008) 6240–6245.
[12] G.O. Phillips, J.C. Arthur Jr., Photochemistry and radiation chemistry of cellulose, in: T.P. Nevell, S.H. Zeronian (Eds.), Cellulose Chemistry and its Applications, Ellis Horwood Ltd. Publishers, Chichester, 1985, p. 291.
[13] T. Toth, J. Borsaa, E. Takacs, Effect of preswelling on radiation degradation of cotton cellulose, Radiat. Phys. Chem. 67 (2003) 513–515.
[14] L. Calucci, C. Pinzono, M. Zandomeneghi, A. Capocchi, Effects of γ-irradiation on the free radical and antioxidant contents in nine aromatic herbs and spices, J. Agric. Food Chem. 51 (2003) 927–934.
[15] H.B. David, L.T. Fan, Y.H. Lee, γ-irradiation as a pretreatment for the enzymatic hydrolysis of cellulose, Biotechnol. Lett. 2 (10) (1980) 435–438.
[16] D.N.-S. Hon, W.G. Glasser, The effect of mechanical action on wood and fiber components, Tappi 62 (10) (1979) 107–120.
[17] R.W. Rex, Electron paramoneuc resonance studies of stable free radicals in lignins and humicacide, Nature 188 (1960) 1185–1186.
[18] M. Foston, Advances in solid-state NMR of cellulose, Curr. Opin. Biotechnol. 27 (2014) 176–184.
[19] J. Bian, F. Peng, X.P. Peng, F. Xu, R.C. Sun, J.F. Kennedy, Isolation of hemicelluloses from sugarcane bagasse at different temperatures: structure and properties, Carbohydr. Polym. 88 (2012) 638–645.